JOURNAL OF THEORETICAL AND APPLIED MECHANICS
51, 4, pp. 859-871, Warsaw 2013

LES-CMC AND LES-FLAMELET SIMULATION OF NON-PREMIXED METHANE FLAME (SANDIA F)

Artur Tyliszczak

Czestochowa University of Technology, Institute of Thermal Machinery, Częstochowa, Poland
e-mail: atyl@imc.pcz.czest.pl

In this paper, the Large Eddy Simulation (LES) together with the Conditional Moment Closure (CMC) and flamelet combustion models have been applied for modelling of methane flame Sandia F. In the case of the CMC model, both instantaneous and time averaged values predicted numerically agree well with measurements. Attention was devoted to modelling aspects of the conditional scalar dissipation rate (SDR), which is a key quantity of the CMC approach. The two methods of computing SDR are compared with emphasis on a correct prediction of localised extinctions and on their influence on the mean values. It was found that the method of modelling of SDR has rather minor impact on the instantaneous values, whereas larger differences were observed in statistics. In the case of the flamelet model, although it is not able to predict extinctions and re-ignition, the mean values were in good agreement with the experiment.

Key words: localised extinction, piloted flame, large eddy simulation, conditional moment closure, flamelet

1. Introduction

The Large Eddy Simulation (LES) method is becoming a standard tool in academic research in virtually all aspects of contemporary CFD (Computational Fluid Dynamics) including reactive flows with combustion. The LES approach, contrary to the classical (u)RANS ((unsteady) Reynolds Averaged Navier-Stokes) methods, gives a very deep insight into the unsteady turbulent flow phenomena. In the case of fundamental research, the LES method is often combined with very sophisticated combustion models such as the Conditional Moment Closure (CMC) (Klimenko and Bilger, 1999) or Eulerian PDF approach (Jones and Prasad, 2010), which are currently regarded as the most accurate. The CMC model applied in this paper allows for analysis of very complicated physical processes including lifted flames (Navarro-Martinez and Kronenburg, 2011), local extinction (Garmory and Mastorakos, 2011), auto-ignition (Stankovic *et al.*, 2011; Tyliszczak, 2013) or forced ignition (Triantafyllidis *et al.*, 2009).

A big disadvantage of the CMC model is very high computational cost both from the point of view of memory requirements as well as from the point of view of computational time. Hence, LES-CMC simulations even for relatively simple problems always involve a number of optimisation steps which in many cases open fields for simplifications and various modelling strategies.

The paper concentrates on modelling aspects of the conditional scalar dissipation rate (wherein after abbreviated as SDR) which is a key parameter of the CMC model. We focus on its influence on time averaged quantities and on correctness of capturing localised extinctions. The test case is a piloted methane flame issuing into ambient air – the so-called Sandia flame. We consider Sandia flame F in which, due to high fuel velocity, the localised extinctions occur in a large extent. Analysis of possible influence of SDR modeling was motivated by Garmory and

Mastorakos (2011) where it was found that proper modelling of Sandia F flame required calibration of the model constant in the formula for SDR. In the present work, rather than tuning the model constant, we compare two different approaches to calculate conditional values of SDR.

Considering the complexity of the CMC approach, on the opposite side there is a flamelet combustion model (Peters, 2000; Poinsot and Veynante, 2001) which is both simple in formulation and very efficient from the computational point of view. Known limitation of the flamelet model is its inability to predict the extinction caused, for instance, by a strong velocity gradient. In this work, the LES-Flamelet approach is applied for purpose of comparison with the CMC method, it is shown that lack of excellent features of the CMC method does not necessarily mean wrong results.

The paper is organised as follows: in the next section presentation of LES and CMC methods is limited to the fundamental formulation and appropriate papers are cited for interested readers; the main attention is paid to possible variants of modelling of the scalar dissipation rate which are then compared in computations; in Section 3 numerical schemes and algorithms used in the LES and CMC codes are briefly characterised; the obtained results are presented in Section 4, which is followed by conclusions.

2. Mathematical modelling

2.1. LES formulation

In LES, the scales of turbulent flow are divided into large scales which are directly solved on a given numerical mesh, and the small scales (subgrid scales) which require modelling. The separation of the scales is obtained by spatial filtering (Geurts, 2003) which applied to the continuity equation, the Navier-Stokes equations and the transport equation for the mixture fraction gives

$$\begin{aligned}
&\frac{\partial \bar{\rho}}{\partial t}+\frac{\partial \bar{\rho}\widetilde{u}_j}{\partial x_j}=0\\
&\frac{\partial \bar{\rho}\widetilde{u}_i}{\partial t}+\frac{\partial \bar{\rho}\widetilde{u}_i\widetilde{u}_j}{\partial x_j}=-\frac{\partial \bar{p}}{\partial x_i}+\frac{\partial \tau_{ij}}{\partial x_j}+\frac{\partial \tau_{ij}^{sgs}}{\partial x_j}\\
&\frac{\partial \bar{\rho}\widetilde{\xi}}{\partial t}+\frac{\partial \bar{\rho}\widetilde{u}_i\widetilde{\xi}}{\partial x_i}=\frac{\partial}{\partial x_i}\Big(\bar{\rho}\mathcal{D}\frac{\partial \widetilde{\xi}}{\partial x_i}\Big)+\frac{\partial J_{sgs}}{\partial x_i}
\end{aligned} \tag{2.1}$$

where the overbar symbol stands for the LES filtering applied to density ($\bar{\rho}$) and pressure ($\bar{p}$). The wide tilde symbol stands for the density weighted filtering applied to the velocity field $\widetilde{u}_i=\overline{\rho u_i}/\bar{\rho}$ and mixture fraction $\widetilde{\xi}=\overline{\rho\xi}/\bar{\rho}$. The mixture fraction is a conserved quantity representing the ratio of the mass fraction of the fuel and oxidiser, and it may be regarded as a quantity reflecting the level of local mixing. The mixture fraction is a key element of the CMC model as well as all types of the *flamelet* based combustion models (Poinsot and Veynante, 2001).

The viscous terms are represented by the tensor $\tau_{ij}=\mu(\partial\widetilde{u}_i/\partial x_j+\partial\widetilde{u}_j/\partial x_i-2/3\delta_{ij}\partial\widetilde{u}_k/\partial x_k)$, and unresolved subgrid stress terms τ_{ij}^{sgs} and J_{sgs} are modelled by the eddy viscosity type model defined as

$$\tau_{ij}^{sgs}=2\mu_t S_{ij}-\frac{1}{3}\tau_{kk}\delta_{ij}\qquad\qquad J_{sgs}=\bar{\rho}D_t\frac{\partial\widetilde{\xi}}{\partial x_i} \tag{2.2}$$

where S_{ij} is the rate of the strain tensor of the resolved field. The subgrid viscosity μ_t is computed according to the model proposed by Vreman (2004) and the subgrid diffusivity is defined as $D_t=\mu_t/\rho\mathrm{Sc}_t$, where Sc_t is the turbulent Schmidt number is assumed constant $\mathrm{Sc}_t=0.4$ (Triantafyllidis and Mastorakos, 2009).

2.2. CMC formulation

The CMC model has been formulated in 90s independently by Klimenko and Bilger and then it was summarized in their joint paper (Klimenko and Bilger, 1999). In the context of LES, the CMC model was presented by Navarro-Martinez *et al.* (2005) approximately ten years later. The LES-CMC model has been derived applying the density-weighted conditional filtering operation (Colucci *et al.*, 1998) to the transport equations for the species mass fraction (Y_k) and total enthalpy. The CMC equations in the framework of LES are given as (Navarro-Martinez *et al.*, 2005; Triantafyllidis and Mastorakos, 2009)

$$\frac{\partial Q_k}{\partial t} + \widetilde{u_i|\eta}\frac{\partial Q_k}{\partial x_i} = \widetilde{N|\eta}\frac{\partial^2 Q_k}{\partial \eta^2} + \widetilde{\dot{\omega}}_k|\eta + e_Y \qquad k = 1, 2, \ldots, n \tag{2.3}$$

where n is the number of species. The operator $(\cdot|\eta) = (\cdot|\xi = \eta)$ is the conditional filtering operator with conditioning being done on the mixture fraction. The symbol $Q_k = \widetilde{Y_k|\eta}$ is conditionally filtered species mass fractions, $\widetilde{u_i|\eta}$ – conditionally filtered velocity, $\widetilde{N|\eta}$ – conditionally filtered SDR, and $e_Y = \frac{\partial}{\partial x_i}(D_t|\eta\frac{\partial Y_k}{\partial x_i})$ represents the subgrid interactions (Triantafyllidis and Mastorakos, 2009). The conditionally filtered reaction rate is evaluated with the 1-st order closure (Klimenko and Bilger, 1999) where the subgrid conditional fluctuations are neglected, i.e. $\widetilde{\dot{\omega}}_k|\eta = \omega_k(Q_1, Q_2, \ldots, Q_n)$. The conditionally filtered variables are related to the filtered variables by integration over the mixture fraction space, this is defined as: $\widetilde{f} = \int_0^1 \widetilde{f|\eta}\widetilde{P}(\eta)\,d\eta$, where $\widetilde{P}$ is the filtered probability density function assumed here as beta-function PDF (Cook and Riley, 1994). We note that the above integral formula is also used in the flamelet model in which the term $\widetilde{f|\eta}$ is replaced by the laminar flamelet solution (Poinsot and Veynante, 2001) obtained solving: $N\frac{\partial^2 Y_k}{\partial \xi^2} + \dot{\omega}_k = 0$ with $N = N_0 G(\xi)$ defined in Eq. (2.4).

The CMC equations are formulated in four-dimensional space, i.e. physical co-ordinates and mixture fraction space. This means that in every time step the solution should have been computed on $N_{x,y,z} \times N_\eta$ nodes, where $N_{x,y,z}$ and N_η denote the number of nodes in the physical and mixture fraction spaces. This leads to a very high computational cost which absolutely prevents application of the LES-CMC approach for realistic problems, and even in simple cases the computations are hardly feasible. A common simplifying approach is to use two separate meshes: one for the solution of the flow field (CFD mesh) and another one, much coarser for the CMC equations (CMC mesh). Although the application of the coarser mesh for the CMC model is a must, it is additionally justified by the fact that in the physical space the conditionally filtered variables are smoother than the LES filtered variables (Navarro-Martinez *et al.*, 2005). Hence, they do not require the numerical resolution as good as for the flow variables (velocity, mixture fraction). In the papers cited in the introduction, the ratio of the nodes of CFD/CMC meshes varies in between 20-300 depending on the flow problem.

The main difficulty of the CMC model is related to the modelling of the conditional terms appearing in Eq. (2.3), i.e. the conditionally filtered SDR, velocity and diffusivity. Among these terms, the most important is the SDR which directly influences on the solution in the mixture fraction space. As it was shown in Triantafyllidis and Mastorakos (2009), Stankovic *et al.* (2011), Garmory and Mastorakos (2011), Tyliszczak (2013) the modelling of $\widetilde{N|\eta}$ may have a crucial impact on the results, and it may qualitatively change the flow behavior.

The application of two meshes causes that the conditional terms have to be first computed based on the resolved variables on the CFD mesh and then transferred to the CMC mesh where the CMC equations are being solved. The conditional velocity and diffusivity are usually expressed directly by the filtered values (Navarro-Martinez *et al.*, 2005; Triantafyllidis and Mastorakos, 2009; Stankovic *et al.*, 2011; Garmory and Mastorakos, 2011), i.e. $\widetilde{u_i|\eta} \approx \widetilde{u}_i$ and $D_t|\eta \approx D_t$,

whereas the SDR is most often computed with the *AMC – Amplitude Mapping Closure* model (Kim and Mastorakos, 2006) defined as

$$\widetilde{N|\eta} = N_0 G(\eta) \qquad G(\eta) = exp\Big(-2[\,\mathrm{erf}^{-1}(2\eta-1)]^2\Big)$$
$$N_0 = \frac{\widetilde{N}}{\int\limits_0^1 G(\eta)\widetilde{P}(\eta)\,d\eta} \tag{2.4}$$

where $\mathrm{erf}\,(x)$ is the error function. The filtered scalar dissipation rate $\widetilde{N}$ is computed as the sum of the resolved and subgrid part (Garmory and Mastorakos, 2011; Navarro-Martinez *et al.*, 2005; Navarro-Martinez and Kronenburg, 2011)

$$\widetilde{N} = \underbrace{\mathcal{D}\Big[\frac{\partial\widetilde{\xi}}{\partial x_i}\frac{\partial\widetilde{\xi}}{\partial x_i}\Big]}_{\text{resolved}} + \underbrace{\frac{1}{2}C_N\frac{\nu_t}{\Delta^2}\widetilde{\xi''^2}}_{\text{subgrid}} \tag{2.5}$$

Following (Triantafyllidis and Mastorakos, 2009; Stankovic *et al.*, 2011; Navarro-Martinez and Kronenburg, 2011), the model constant is assumed $C_N = 2$, although different values may be found in literature (Garmory and Mastorakos, 2011; Tyliszczak, 2013). There are no clear pieces of advice what value of C_N should be in a particular problem, and thus the value of C_N is sometimes estimated based on existing experimental or DNS data, or sometimes it is set by trial and error. This paper does not aim to calibrate C_N, and we rather focus on a methodology of calculation of conditional SDR on the CMC mesh. As it was mentioned, the application of two meshes requires that the conditional terms computed on the CFD mesh must be transferred to the CMC mesh. Various possibilities for transferring data between the CMC and CFD meshes were discussed in Triantafyllidis and Mastorakos (2009). Assuming that the conditional variables ($\widetilde{f|\eta}$) have been computed on the CFD mesh, their counterparts on the CMC mesh are calculated by using a PDF weighted volume integral within the CMC cells (V_{CMC}) to which $\widetilde{f|\eta}$ belong. This is defined as

$$\widetilde{f|\eta}^{\,*} = \frac{\int\limits_{V_{CMC}} \bar{\rho}\widetilde{P}(\eta)\widetilde{f|\eta}\,dV'}{\int\limits_{V_{CMC}} \bar{\rho}\widetilde{P}(\eta)\,dV'} \tag{2.6}$$

Thus, the conditionally filtered variable $\widetilde{f|\eta}^{\,*}$ corresponding to the CMC cell is common for a group of the CFD nodes embedded in that CMC cell. Formula (2.6) is applied for the velocity $\widetilde{u_i|\eta}^{\,*}$, diffusivity $\widetilde{D_t|\eta}^{\,*}$ and also for the scalar dissipation rate $\widetilde{N|\eta}^{\,*}$. However, in this case we additionally tested another option to compute $\widetilde{N|\eta}^{\,*}$, i.e. we applied the AMC model directly on the CMC resolution (Triantafyllidis and Mastorakos, 2009). This approach leads to

$$\widetilde{N|\eta}^{\,*} = N_0^* G(\eta) \qquad N_0^* = \frac{\widetilde{N}^*}{\int\limits_0^1 G(\eta)\widetilde{P}^*(\eta)\,d\eta} \tag{2.7}$$

where $\widetilde{N}^*$ and $\widetilde{P}^*(\eta)$ are the volume integrated values

$$\widetilde{N}^* = \frac{\int\limits_{V_{CMC}} \bar{\rho}\widetilde{N}\,dV'}{\int\limits_{V_{CMC}} \bar{\rho}\,dV'} \qquad \widetilde{P}^*(\eta) = \frac{\int\limits_{V_{CMC}} \bar{\rho}\widetilde{P}(\eta)\,dV'}{\int\limits_{V_{CMC}} \bar{\rho}\,dV'} \tag{2.8}$$

In this work we compare the results obtained with two variants of computing $\widetilde{N|\eta}^*$. The model defined by Eq. (2.4) with volume integration according to Eq. (2.6) will be denoted as *N-1*, and the model defined by Eq. (2.7) with Eq. (2.8) will be denoted as *N-2*.

Having the conditional terms computed on the CMC mesh, the CMC equations may be then solved. Next, using the conditionally filtered variables the LES filtered variables, on the CFD mesh are obtained from

$$\widetilde{f}(x,t) = \int_0^1 \widetilde{f|\eta}^* \widetilde{P}(\eta)\, d\eta \tag{2.9}$$

with $\widetilde{P}(\eta)$ evaluated separately in each CFD node and with $\widetilde{f|\eta}^*$ being the same for a group of the CFD nodes sharing particular CMC cells.

3. Numerical methods

The CMC and flamelet models have been implemented in a high-order LES solver called SAILOR. The SAILOR code is based on the low Mach number approach (Cook and Riley, 1996). The spatial discretisation is performed by the 6th order compact method (Lele, 1992) for the Navier-Stokes and continuity equations and with 5th order WENO scheme (Shu, 2003) for the mixture fraction. The time integration is performed by the Adams-Bashforth/Adams-Multon predictor-corrector approach. The solution algorithm is well verified, the SAILOR code was used in various LES studies for gaseous flows, multi-phase flows and flames (Kuban *et al.*, 2010, 2012; Aniszewski *et al.*, 2012; Tyliszczak, 2013).

The CMC equations were solved applying the operator splitting approach where the transport in a physical space, transport in a mixture fraction space and chemistry are solved separately. In the physical space, the conditional variables are smoother than the filtered ones (Navarro-Martinez *et al.*, 2005; Triantafyllidis and Mastorakos, 2009), and hence, without significant loss of accuracy, the CMC equations could be discretised using the second order finite difference method combined with 2nd order TVD (Total Variation Diminishing) scheme with van Leer limiters for the convection terms (Hirsch, 1990). The TVD schemes guarantee stable solutions without unphysical oscillations that could have appear in regions of strong gradients – for instance in the vicinity of locally extinguishing or re-igniting flame. The time integration within the operator splitting approach consists of three steps. First, the system resulting from the spatial discretisation in the physical space is solved applying the first order explicit Euler method. In the mixture fraction space, the CMC equations are stiff due to the reaction rate terms. In this case, the time integration is performed applying the implicit Euler method combined with VODPK (Brown and Hindmarsh, 1989) solver that is well suited for stiff systems. The reaction rates were computed using CHEMKIN interpreter.

In this work, we used two well known chemical mechanisms: the Smooke mechanism (Smooke, 1991) with 16 species and 25 reactions and the GRI-2.11 chemical mechanism (Bowman *et al.*, [3]) containing 49 species reacting through 277 elementary reactions. The Smooke mechanism was applied both for the CMC and flamelet models, whereas the GRI-2.11 mechanism was used with the flamelet model only. As the flamelet model is computationally very efficient comparing to the CMC approach, it allowed for using much more sophisticated chemistry. On the other hand, the simulations with the CMC model and with the GRI-2.11 chemistry would probably take tremendous amount of time, e.g. the computations (initial flow evolution and gathering statistics) with the Smooke mechanism took 5 days for the flamelet model, whereas for the CMC model almost 30 days were needed. In the following Section, the presentation of the results obtained by applying the flamelet model is limited to those obtained with the GRI-2.11 mechanism as it is regarded as more accurate.

4. Computational results

The Sandia flames (Barlow and Frank, 1998) are commonly used test cases for non-premixed combustion models and are probably the most often computed flames over the world. Sketch of the computational configuration is shown in Fig. 1 on the left hand side. The nozzle consists of the inner fuel pipe with a diameter $D = 7.2\,\text{mm}$ and the outer pipe with a diameter $D = 18.2\,\text{mm}$ for the pilot flame. The fuel jet is a mixture of methane and air with mass fractions $Y_{CH_4} = 0.156$, $Y_{O_2} = 0.197$, $Y_{N_2} = 0.647$, what corresponds to the stoichiometric mixture fraction $\xi_{ST} = 0.351$. The total amount of oxygen is small and insufficient for combustion and, therefore, this flame is classified as non-premixed. The pilot flame corresponds to the mixture fraction $\xi = 0.27$ and was modelled assuming the steady flamelet solution. The temperature of the fuel jet and coflowing air is equal to 300 K and their velocities are $U_j = 99.2\,\text{m/s}$ and $U_c = 1.0\,\text{m/s}$.

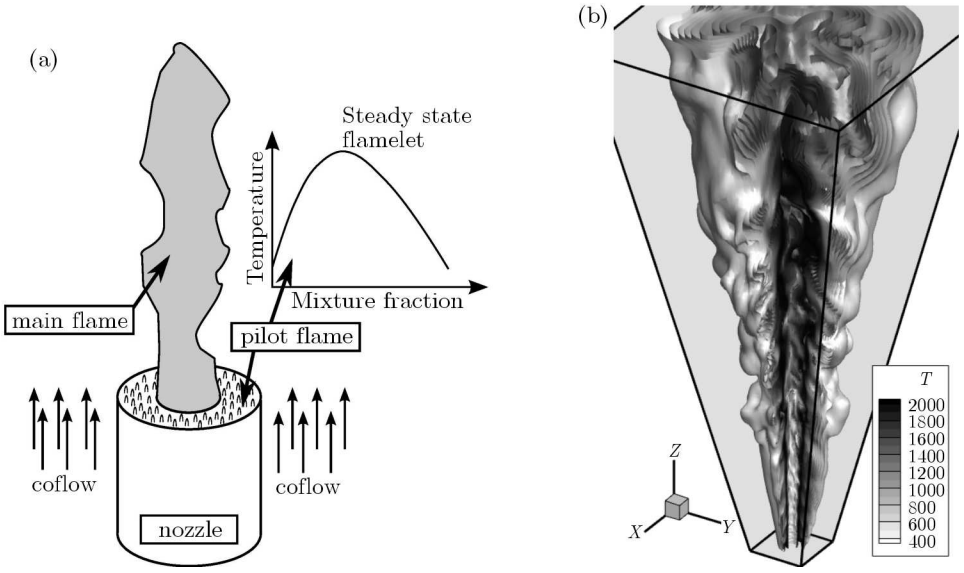

Fig. 1. Schematic view of the nozzle for Sandia flames (a) and the isosurfaces of instantaneous temperature (b)

Preliminary computations were necessary in order to set-up the computational domain and meshes ensuring a sufficient resolution. Various cuboidal or hexahedral shapes with meshes consisting of various number of nodes and stretching parameters were analysed. Finally, the computational domain had a hexahedral shape with dimensions: length 60D, inlet plane $6D \times 6D$ and outlet plane $30D \times 30D$. The CFD mesh consisted of $128 \times 216 \times 128$ nodes and the CMC mesh was much coarser with $20 \times 40 \times 20$ nodes. In both cases, the meshes were slightly stretched axially and radially towards the nozzle. The inlet boundary conditions were specified in terms of the velocity and mixture fraction and they corresponded to the experimental profiles (Barlow and Frank, 1998). The lateral boundaries were also assumed as the inlet with zero mixture fraction and axial velocity equal to U_c. The outlet boundary was assumed as a convective outflow with constant pressure. The boundary conditions in the physical space for the conditional variables were specified in terms of solutions in the mixture fraction space, i.e. in every node at the boundary the solution for Q_k is given the entire range $0 \leqslant \xi \leqslant 1$; (i) at the inlet plane in the regions of the fuel jet and coflow the inert solution was assigned, i.e. it was assumed that the species and enthalpy vary linearly for $0 < \xi < 1$; in the region of the pilot flame the steady flamelet corresponding to burning state was defined (shown schematically in Fig. 1); (ii) all remaining boundaries are assumed as the Neumann boundary conditions.

4.1. Instantaneous results

The Sandia flame F corresponds to a fully developed turbulent flame, the complexity of the flow structure represented by isosurfaces of the temperature is shown in Fig. 1 on the right hand side. Strongly unsteady flame behaviour is manifested by the occurrence of local extictions which may be well seen in instantaneous experimental data or in numerical results provided that the combustion model predicts the extinction phenomena properly. Figure 2 presents instantaneous contours of the temperature and isoline of the stoichiometric mixture fraction $\xi_{ST} = 0.351$. The CMC results in Fig. 2 are presented together with the solutions obtained applying the steady flamelet model.

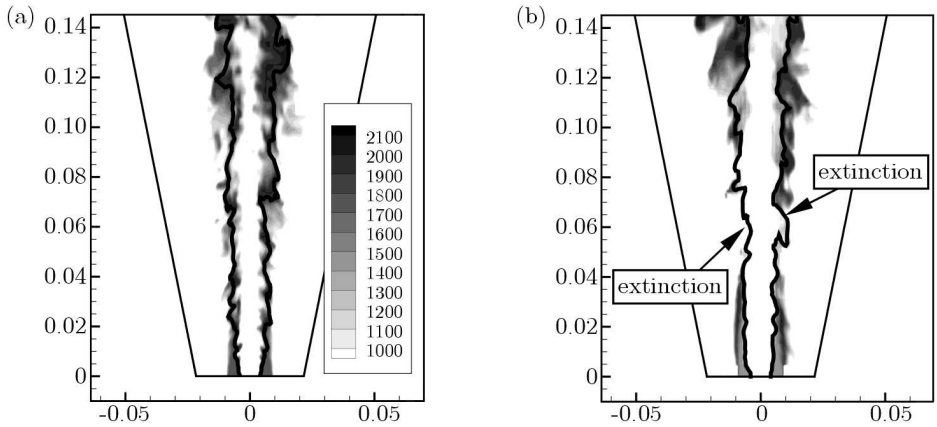

Fig. 2. Contours of instantaneous temperature obtained with the flamelet model (a) and the CMC model (b). The arrows point local instantaneous extinctions

The contours of temperature in Fig. 2 are plotted for values above 900 K. Analysing the results obtained with the flamelet, we can see that for the stoichiometric conditions (black line) the temperature is always high. On the other hand, one may notice that for the CMC results in some points (shown by the arrows) the temperature is low (i.e. < 900 K) even if the mixture is at stoichiometry - such behaviour is interpreted as local extinction. A very good method of quantifying the amount of extinctions is to represent the time variation of a given variable (temperature or species) as the function of the mixture fraction in scatter plots. Such results for the temperature at $z/D = 15$ for the CMC solution with conditional SDR computed according to the method *N-1* and for the flamelet solutions with maximum SDR equal to $N_0 = 2$ and $N_0 = 20$ (see Eq. (2.4)) are shown in Fig. 3. The CMC results obtained applying the method *N-2* are qualitatively not distinguishable from those obtained applying the method *N-1*, and in both cases they remind closely the experimental data. On the other hand, the results from the flamelet model differ from each other and also from the experimental results. As one may observe, the instantaneous values lie close to some *a priori* determined lines, and indeed they correspond to laminar flamelets computed for $N_0 = 2$ and $N_0 = 20$. The small dispersions from these laminar solutions are caused only by the mixture fraction variance. We note that the computations with the Smooke mechanism led to very similar qualitative behaviour, i.e. the dispersion form the laminar flamelets was very small. Hence, as expected, the obtained results clearly illustrate that the flamelet model is unable to predict extinction and, on the other hand, the CMC approach does that very well. This is further confirmed in Fig. 4 showing a comparison of the scatter plots of CO species obtained from the measurements and from simulations applying the CMC with the methods *N-1* and *N-2*. The agreement with the experiment is very good with respect to both the absolute values and distribution and, as one may see, the methods *N-1* and *N-2* give very similar solutions. Finally, one should mention that further downstream or closer to the nozzle the scatter plots from the CMC results also agree reasonable well with the experiment.

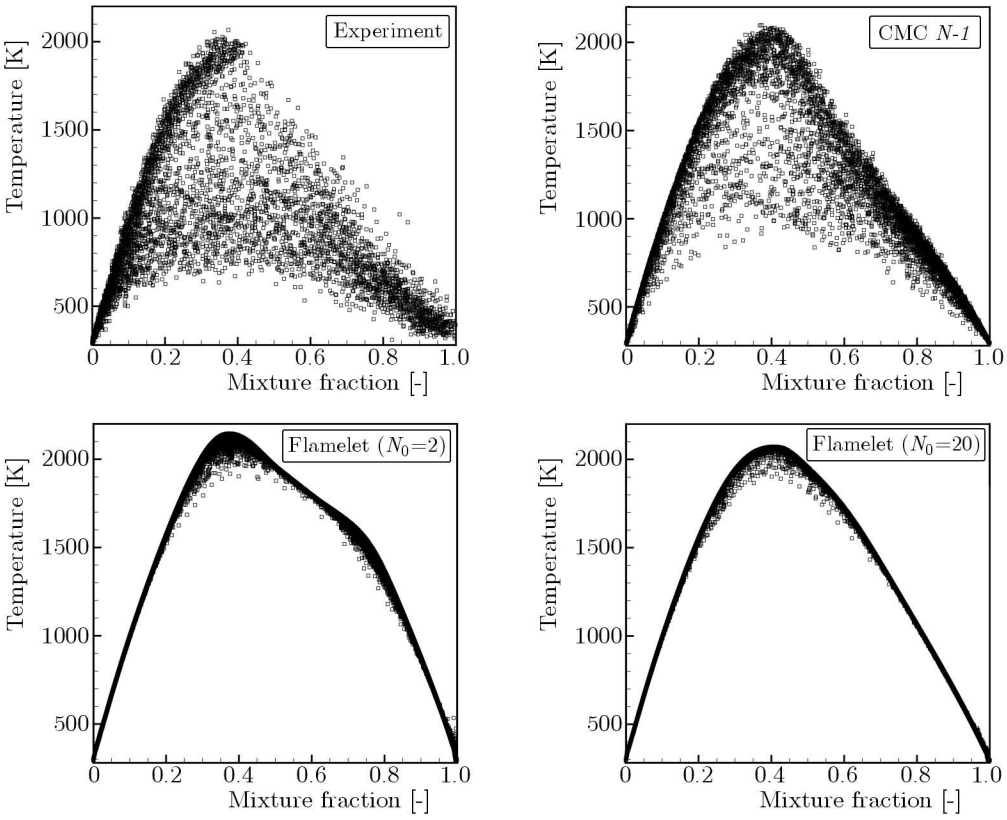

Fig. 3. Scatter plots of temperature at $z/D = 15$. Experimental data and numerical solutions obtained with the CMC model ($\widetilde{N|\eta}$ from *N-1*) and with the flamelet approach for $N_0 = 2$ and $N_0 = 20$

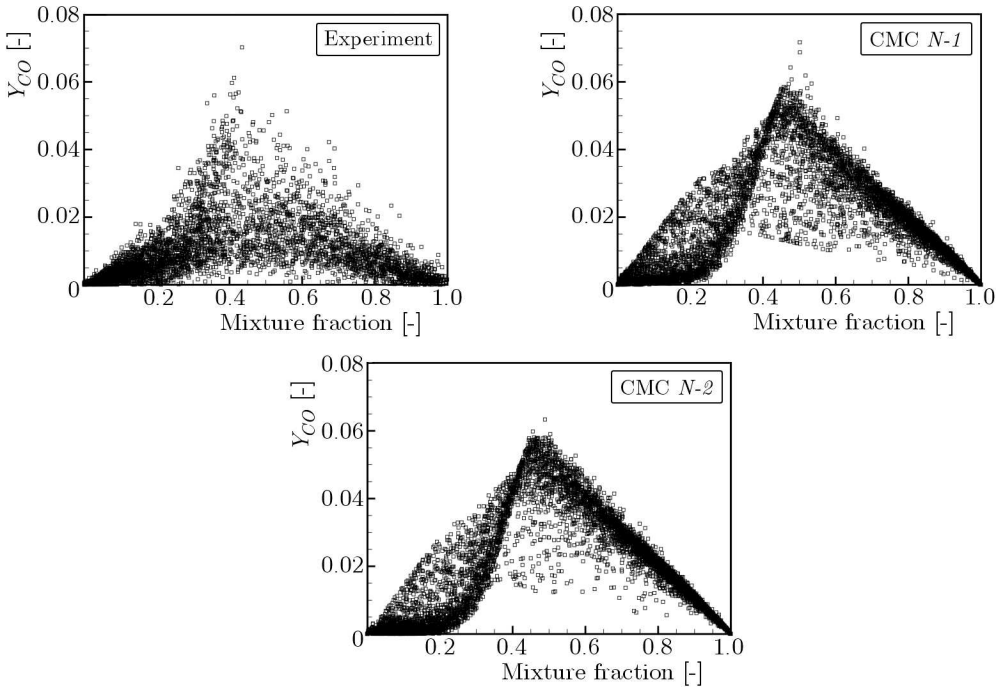

Fig. 4. Scatter plots of the CO mass fraction at $z/D = 15$. Experimental data and numerical soulutions obtained with the CMC solutions model ($\widetilde{N|\eta}$ from *N-1* and *N-2*)

4.2. Averaged results

The instantaneous results have shown that the CMC model predicts local extinctions properly whereas the flamelet model fails in this type of analysis. Below we analyse how this deficiency influences time averaged results. Figures 5-8 show mean profiles of the mixture fraction and temperature together with their fluctuations along the radial direction in four locations from the nozzle $z/D = 7.5$, 15, 30, 45. In these figures, the results obtained with the CMC model are presented for two variants of computing $\widetilde{N|\eta}$. They are compared with solutions obtained using the flamelet model with $N_0 = 20$ and with the experimental data. The results for the flamelet model with $N_0 = 2$ are not much different from those for $N_0 = 20$. Depending on the location and compared quantity, the results for $N_0 = 2$ are slightly better or slightly worse with respect to the experiment.

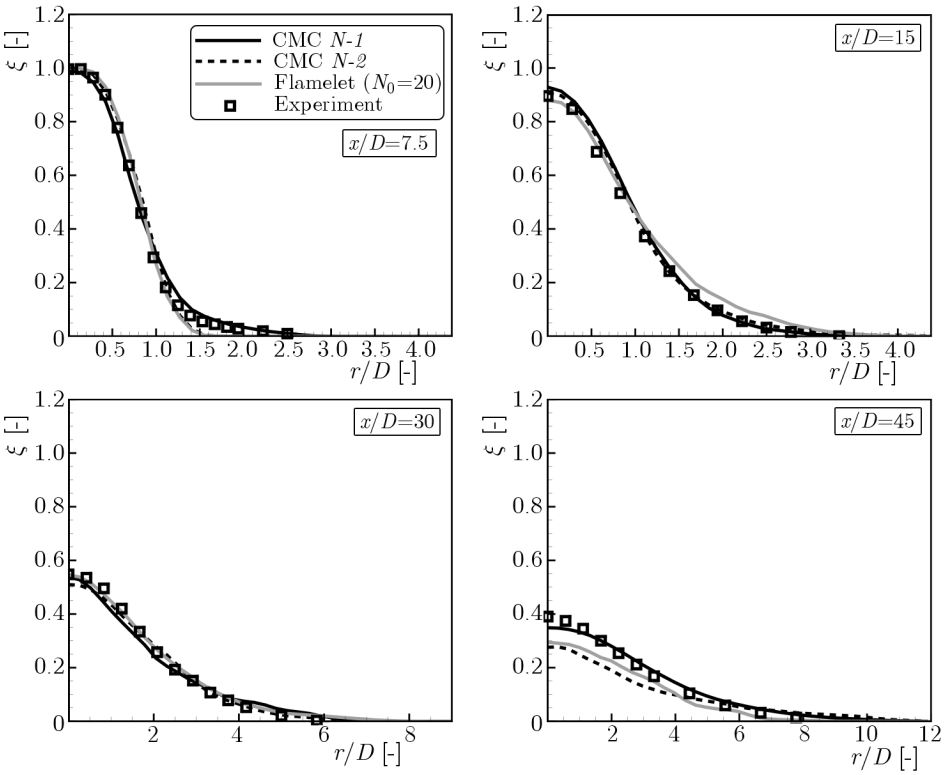

Fig. 5. Radial profiles of the mean mixture fraction at selected locations from the nozzle

The CMC results obtained applying the method *N-1* or *N-2* differ substantially from each other. From all presented results those corresponding to *N-1* are in the best agreement with the experiment, although the remaining solutions are also accurate. Hence, there are two interesting findings: (i) firstly, it seems that inability to predict local extinction by the flamelet model has no crucial influence on the time averaged results; this would mean that the local extinctions in the analysed flame are very short lasting phenomena whoose overall duration is small compared to time when the mixture burns; (ii) the instantaneous CMC results applying the method *N-1* or *N-2* were very similar but it was not the case for the time averaged values; this means that the way how the conditional SDR is computed has larger impact on statistics than instantaneous values. To some extent, this is in contradiction with the results presented by Garmory and Mastorakos (2011), where they stressed the importance of $\widetilde{N|\eta}$ with respect to modeling of instantaneous values. They used the method *N-2*, and in order to predict local extinctions correctly, they calibrated the level of $\widetilde{N|\eta}$ using experimental data for Sandia D flame, eventually they used the model constant $C_N = 42$ in Eq. (2.5). Unfortunately, they did not show how the level of

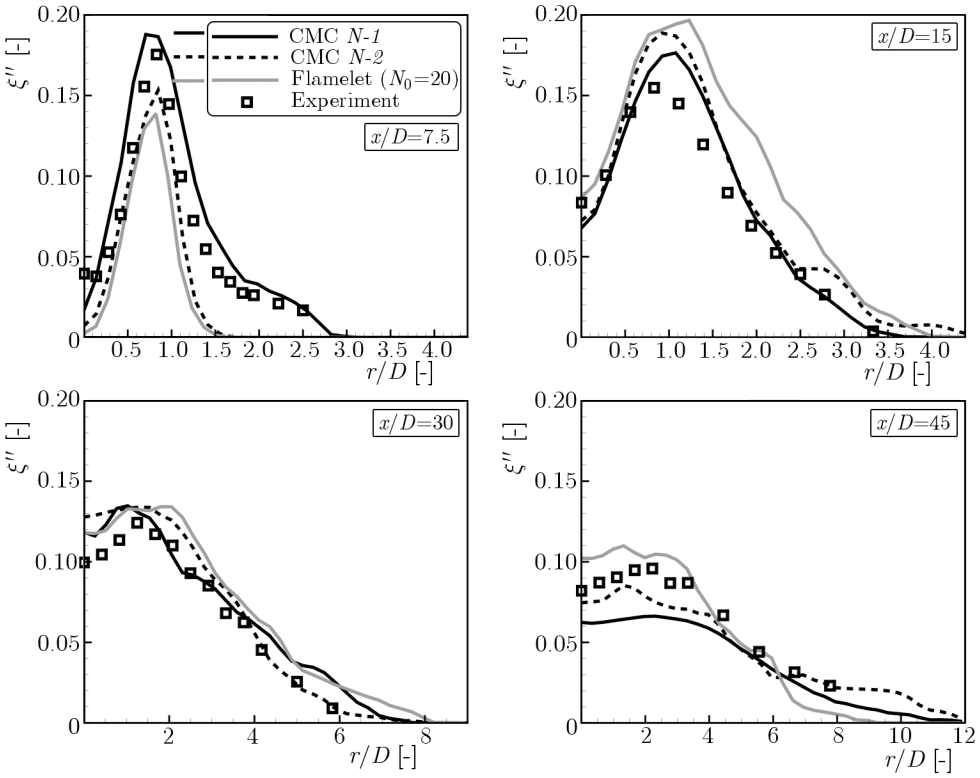

Fig. 6. Radial profiles of the mixture fraction RMS at selected locations from the nozzle

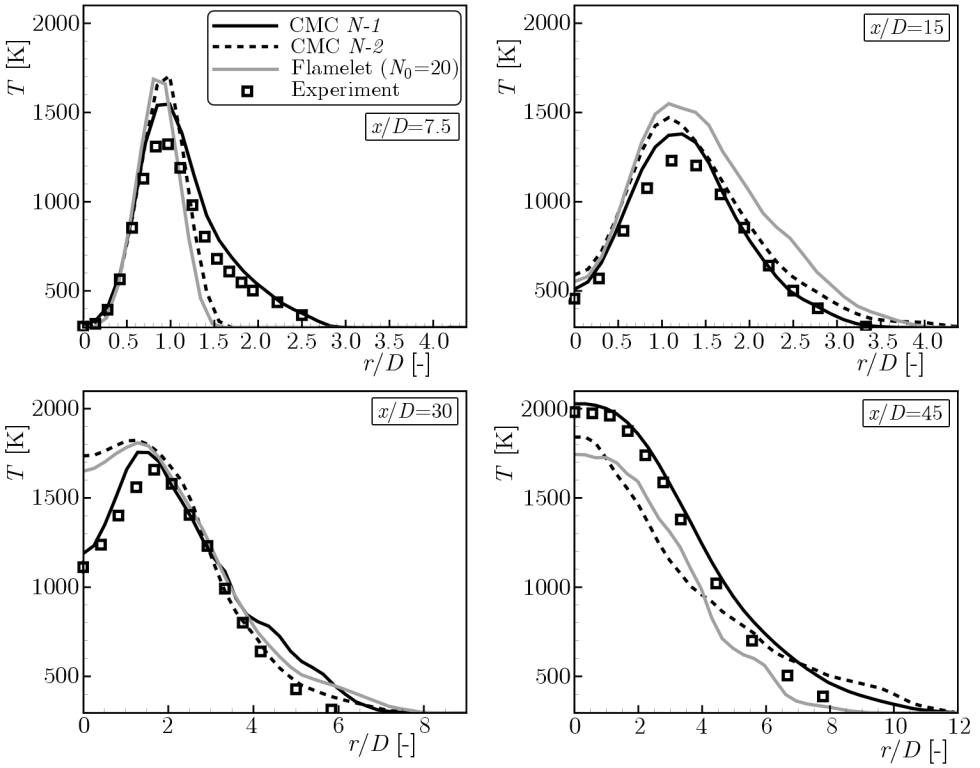

Fig. 7. Radial profiles of the mean temperature at selected locations from the nozzle

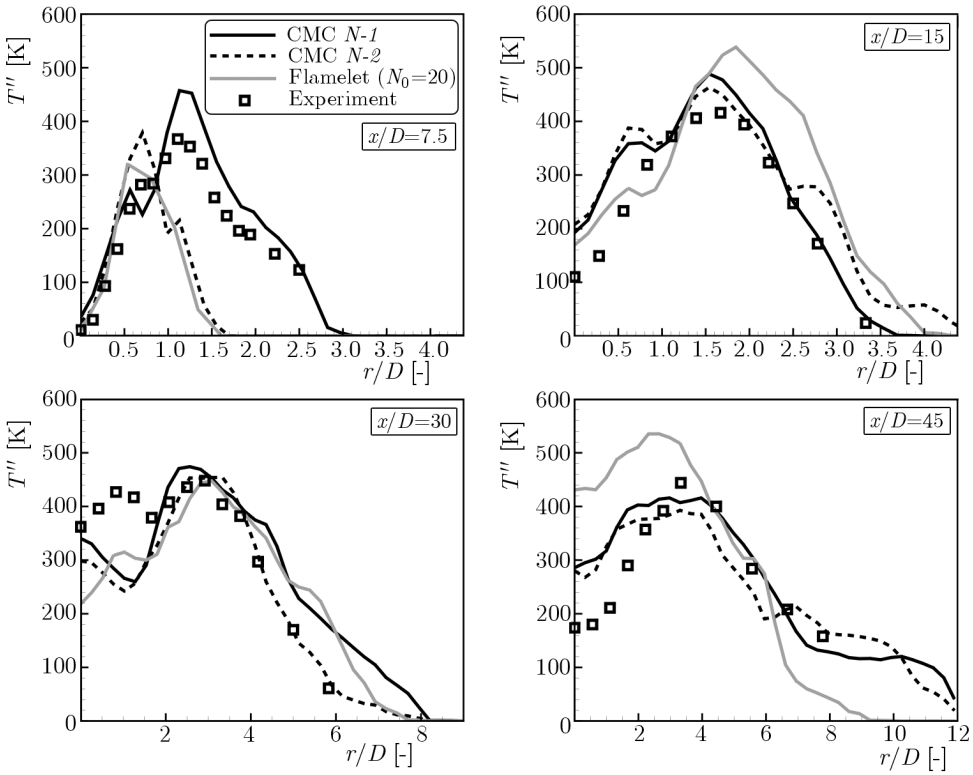

Fig. 8. Radial profiles of the temperature RMS at selected locations from the nozzle

$\widetilde{N|\eta}$ influences the mean values and what are instantaneous values of the temperature or species for different $C_N = 42$. The present solutions show that from the point of view of the time averaged results, the method *N-1* gives better results than the method *N-2*, and hence, one may suppose that calibration of the model constant for $\widetilde{N|\eta}$ in Eq. (2.4) would produce even better predictions. That analysis is planned for future research.

5. Conclusions

The LES-CMC and LES-Flamelet approaches have been successfully applied to the modelling of non-premixed methane flame (Sandia F). The experimental data show that due to high fuel velocity the flame locally extinguishes and re-ignites. Numerical modelling of such phenomena is a challenging task for all combustion models and only few are able to model them correctly. As shown in the cited papers and in the present work, the CMC approach allows for analysis of the extinction and re-ignition with good accuracy. The formulation of the CMC model is very complex both from the theoretical point of view as well as from the computational side where the main issue is related to very high computational cost forcing the application of two different meshes: dense mesh for the LES solver and coarse mesh for the CMC. This, in turn requires a transfer of variables between CFD and CMC mesh. In this paper, it was shown that the method of transferring the conditional scalar dissipation rate may have significant influence on time averaged values and relatively minor on instantaneous values. These results are surprising and certainly need further analysis. Another important and interesting observation is that the flamelet model, which completely fails in the simulation of local extinction, gives averaged values in the acceptable agreement with the experimental data. So, taking into account the computational cost of the CMC model, one should always consider application of the flamelet approach, particularly when a very deep insight in flow physics is not the main task and when

the instantaneous phenomena do not determine the flow behaviour. On the other hand, if the oposite is the case, the CMC approach is indispensable.

Acknowledgements

The financial support for this work was provided by the Polish Ministry of Science under grant N N501 098938. This research was supported in part by PL-Grid Infrastructure. The author thanks to Prof. E. Mastorakos for extensive discussions on the CMC model.

References

1. Aniszewski W., Boguslawski A., Marek M., Tyliszczak A., 2012, A new approach to subgrid surface tension for LES of two-phase flows, *Journal of Computational Physics*, **231**, 7368-7397
2. Barlow R.S., Frank J.H., 1998, Effect of turbulence on species mass fractions in methane/air jet flames, *Proceedings of the Combustion Institute*, **27**, 1087-1095
3. Bowman C.T., Hanson R.K., Davidson D.F., Gardiner W.C. Jr., Lissianski V., Smith G.P., Golden D.M., Frenklach M., Goldenberg M., *Description of the GRI mechanisms*, http://www.me.berkeley.edu/gri_mech/
4. Brown P.N., Hindmarsh A.C., 1989, Reduced storage matrix methods in stiff ODE systems, *Journal of Computational Physics*, **31**, 40-91
5. Colucci P.J., Jaberi F.A., Givi P., Pope S.B., 1998, Filtered density function for large eddy simulation of turbulent reacting flows, *Physics of Fluids*, **10**, 499-515
6. Cook A.W., Riley J.J., 1994, A subgrid model for equilibrium chemistry in turbulent flows, *Physics of Fluids*, **6**, 2868-2870
7. Cook W.C., Riley J.J., 1996, Direct numerical simulation of a turbulent reactive plume on a parallel computer, *Journal of Computational Physics*, **129**, 263-283
8. Garmory A., Mastorakos E., 2011, Capturing localised extinction in Sandia flame F with LES-CMC, *Proceedings of the Combustion Institute*, **33**, 1673-1680
9. Geurts B.J., 2003, *Elements of Direct and Large-Eddy Simulation*, Edwards Publishing
10. Hirsch Ch., 1990, *Numerical computation of internal and external flows*, John Wiley & Sons, Chichester
11. Jones W.P., Prasad V.N., 2010, Large eddy simulation of the Sandia flame series (D, E and F) using the Eulerian stochastic field method, *Combustion and Flame*, **157**, 1621-1636
12. Kim I.S., Mastorakos E., 2006, Simulations of turbulent non-premixed counterflow flames with first order conditional moment closure, *Flow, Turbulence and Combustion*, **76**, 133-162
13. Klimenko Y.A., Bilger R.W., 1999, Conditional moment closure for turbulent combustion, *Progress in Energy and Combustion Science*, **25**, 595-687
14. Kuban L., Laval J.-P., Elsner W., Tyliszczak A., Marquillie M., 2012, LES modeling of converging-diverging turbulent channel flow, *Journal of Turbulence*, **13**, 1-19
15. Kuban L., Tyliszczak A., Boguslawski A., 2010, LES modelling of methane ignition using Eulerian stochastic fields approach, *Proceedings 8th International Symposium on Engineering Turbulence Modelling and Measurements*, **2**, 492-497
16. Lele S.K., 1992, Compact finite difference with spectral-like resolution, *Journal of Computational Physics*, **103**, 16-42
17. Navarro-Martinez S., Kronenburg A., 2011, Flame stabilization mechanism in lifted flames, *Flow, Turbulence and Combustion*, **87**, 377-406
18. Navarro-Martinez S., Kronenburg A., di Mare F., 2005, Conditional moment closure for large eddy simulations, *Flow, Turbulence and Combustion*, **75**, 245-274

19. Peters N., 2000, *Turbulent Combustion*, Cambridge University Press

20. Poinsot T., Veynante D., 2001, *Theoretical and Numerical Combustion*, Edwards

21. Shu C.W., 2003, High-order finite difference and finite volume WENO schemes and discontinuous Galerkin methods for CFD, *Journal of Computational Physics*, **17**, 2, 107-118

22. Smooke M.D., 1991, *Lecture Notes in Physics*, **384**, chapter: *Reduced Kinetic Mechanisms and Asymptotic Approximations for Methane-Air Flames*, p. 23, Springer-Verlag

23. Stankovic I., Triantafyllidis A., Mastorakos E., Lacor C., Merci B., 2011, Simulation of hydrogen auto-ignition in a turbulent co-flow of heated air with LES and CMC approach, *Flow, Turbulence and Combustion*, **86**, 689-710

24. Triantafyllidis A., Mastorakos E., 2009, Implementation issues of the conditional moment closure in large eddy simulations, *Flow, Turbulence and Combustion*, **84**, 481-512

25. Triantafyllidis A., Mastorakos E., Eggels R.L.G.M., 2009, Large Eddy Simulations of forced ignition of a non-premixed bluff-body methane flame with Conditional Moment Closure, *Combustion and Flame*, **156**, 2328-2345

26. Tyliszczak A., 2013, Assessment of conditional scalar dissipation models in LES-CMC simulation of auto-ignition of hydrogen jet, *Archives of Mechanics*, **65**, 2, 97-129

27. Vreman A.W., 2004, An eddy-viscosity subgrid-scale model for turbulent shear flow: Algebraic theory and applications, *Physics of Fluids*, **16**, 3670-3681

Manuscript received October 15, 2012; accepted for print January 28, 2013